

# Influence of wind speed on rain-based attenuation at Ku-band for earth-satellite links in Nigeria

Joseph Sunday Ojo<sup>1</sup>, Isaac Olawale. Sunday<sup>1</sup>, Elijah Olusayo Olurotimi<sup>2</sup>

<sup>1</sup>Department of Physics, The Federal University of Technology, Akure, Nigeria

<sup>2</sup>Department of Electronic Engineering, Durban University of Technology, Durban, South Africa

## Article Info

### Article history:

Received Jun 12, 2022

Revised Nov 8, 2022

Accepted Nov 19, 2022

### Keywords:

Fade mitigation technique

Ku-band satellite services

Quality of service

Rain-influenced attenuation

Synthetic storm technique

Tropical location

Wind speed

## ABSTRACT

The peculiarity of the tropical climate shows that when the quality of service (QoS) on Satellite-Earth propagation links is to be determined, the statistics of rain-based attenuation (RbA), storm speed, and their impacts are the important parameters to be considered, especially at frequencies above 10 GHz. This paper assesses the influence of storm speed in estimating RbA at Ku-band, based on 2-year rain rate data obtained using automatic weather station (AWS) and RbA beacon measurements in Nigeria. The rain rates based on the time series were employed to deduce the time series RbA based on the synthetic storm technique (SST) algorithm. The results show a seasonal pattern of rain rate that correlates with the SST-based RbA. The RbA generated closely follows suit with the beacon measurement, especially under low wind speed, and outperforms the international telecommunications union–radiocommunication sector (ITU-R) model based on the lowest metric measures. However, at a higher storm speed, the RbA generated deviated widely from the measured RbA values by about 16%. These results are crucial for figuring out what needs to be done to protect QoS in a tropical area where wind and rain are common.

*This is an open access article under the [CC BY-SA](https://creativecommons.org/licenses/by-sa/4.0/) license.*



## Corresponding Author:

Joseph Sunday Ojo

Department of Physics, The Federal University of Technology

P.M.B 704, Akure, Nigeria

Email: ojojs\_74@futa.edu.ng

## 1. INTRODUCTION

The advantages of the Ku-band satellite services cannot be exhausted, as it serves as the gateway to high data and video transmission via digital satellite television (such as directly to homes) across the globe. It can be used for both digital satellite television and satellite television broadcasts. The Ku-band is one of the preferred choices in very small aperture terminals (VSATs) technology. The VSAT is one of the best emergency communication backup systems during disasters [1]. Also, the Ku-band employs a VSATs network based on a two-way ground station that sends and accepts data via satellites. The ground-based receiver uses a small dish with low noise blocks (LNBS) for reception focused directly on an elevation angle to receive the signal from the satellite.

However, a signal via the slant path is susceptible to attenuation due to atmospheric hydrometeors, especially rain, among others [2], [3]. It's widely known that rain among other hydrometeor parameters poses a serious degradation to radio waves, which is one of the major problems in earth-satellite systems, especially from 10 GHz and above [2], [4]-[14]. Several studies have also revealed that the rain-based attenuation (RbA) increases with increasing operating frequency and may cause the transmitted signals to be absorbed, scattered, or partially transmitted through the rain medium [6], [15], [16]. As a result of the degradation of signals due to rain, the strength of the received signals can be reduced, resulting in a total loss, and consequently becomes

unavailable for a great percentage of the time in a year [14], [17]. These signal degradations are usually common on the earth-satellite links, especially in tropical regions where high-intensity rainfall are usually experienced [18], [19]. Studies revealed that there is a tendency for high-intensity rain to fall for several hours and may be associated with thunderstorms and high storms in the tropics [6], [15], [20]. Actually, due to the peculiarities of the tropical climate in the determination of quality of service (QoS), the characterization of rain rate statistics in terms of cumulative distribution or yearly distribution may not be enough to fully determine the impact of precipitation on satellite-earth links [21].

The peculiarities of storm speeds in the tropics are also significant for weather determination throughout the region. This may invariably further add to the attenuation of signals travelling from the satellite along the slant path to the end-users. Ogunjo *et al.* [22] investigated the speed and direction of wind speed for Akure, a tropical location in Nigeria. Their results show a noticeable pattern, especially during the dry and wet seasons. However, due to the perceived but unreported fluctuations and unpredictability of wind speed, studies on wind speed as related to signal attenuation have not received much attention, especially in the tropics with many occurrences of storm speed. It is therefore expedient that more knowledge of the wind direction and wind speed as a function of the season is needed to characterize rain fade in satellite communication links [23]. Also, the knowledge of the influence of wind speed on attenuation over the communication links is imperative for proper planning, designing, and optimizing both the received and transmitted propagated signals along the slant path [18], [24], [25]. Moreover, the aftermath of the unavailability of the signals usually affects several other daily activities associated with broadcasting over Ku-band, such as real-time news, automatic teller machine (ATM) services, sports events, movies, and internet services, among others. Hence, it is crucial to further evaluate these features and their impact on Earth-satellite links over a tropical location.

Most of the earlier studies on this subject have focused on the temperate and equatorial regions [6], [15], [16] with little or no focus on tropical regions like Nigeria. The wind-related studies in Nigeria have always been based on weather forecasts and environmental-related problems [22]. However, much work has been done on attenuation-related problems in the tropics as evident in literature [6], [15], [16]. Hence, the need to further evaluate the effect of storm speed on earth-satellite links over the tropical environment.

This study aims to investigate the influence of storm speed in estimating RbA in the Ku-band based on two years (2018 and 2019) of 1-minute rain rate data obtained through the automatic weather station (AWS) rain gauge and RbA from beacon measurements at the Federal University of Technology Akure, Nigeria. These are important for figuring out what needs to be done to protect QoS in a tropical area where wind and rain are common. The rest of the paper is arranged as shown in: the information on the location of the study and the experimental setup is presented in Section 2, the methodology adopted is presented in Section 3, Section 4 discusses the results generated, and the conclusion is presented in Section 5.

## 2. METHOD

The methodology adopted in this work is presented in this section. It primarily presents the RbA system's relevant tools as well as how a high quality of service can be achieved at Ku-Band for earth-satellite links in Nigeria. The section includes information about the study site, experimental setup, data processing, and a description of the synthetic storm techniques.

### 2.1. Study location and experimental setup

The study city for this work is Akure, Nigeria. Akure city is the state capital of Ondo State, which lies between Latitude 7.17° N and Longitude 5.18° E at an altitude of about 358 m above sea level [26], [27]. The city belongs to the tropical region of the rainforest part of Nigeria. The rain-bearing nature of the region was influenced by the Atlantic Ocean and the dry northwest winds from the Sahara Desert. As a rain-bearing region, it is characterized by both hot and humid areas, influenced by the southwestern monsoon winds [25]. As part of the tropics, the city is also characterized by two main seasons: rainy (between April and October), and dry (the rest of the calendar year) [25].

The experimental setup is sited at the Department of Physics, Federal University of Technology, Akure, (7.3070° N, 5.1398° E), Nigeria. The storm speed, storm direction and the rain rate time series were measured concurrently with the received signal from a beacon measurement for 2 years (2018 and 2019). The setup comprises outdoor and indoor units. The outdoor unit consists of a dish and an automatic weather station, (AWS) located beside the Departmental building, while the indoor unit comprises an integrated sensor suite with a data logger, a personal computer for user interface, SATlink and a spectrum analyser located in the communication research lab (CRL), within the departmental building.

The Ku-band signal from the satellite was received by a micro-parabolic antenna 0.9 m in diameter (with a gain of 40 dB) from a horizontally polarized EUTELSAT W4/W7 (036°), at 12.245 GHz with a signal rating of 27,509 bps. The ground-based receiver looked-up angle was set at about 53.2° via the down converter.

The Ku signal from the satellite is converted to an intermediate frequency (IF) range from 950 kHz to 2150 kHz via the low noise block (LNB) attached to the antenna via the looked-up angle. The indoor unit received the output signal of the converter and fed it into the SATlink and a spectrum analyser for further analysis. The output signal is sent to the data logger linked to the computer. The received radio frequency (RF) signal of 12.245 GHz was sampled for several minutes successively at each rain rate to capture the actual reading. The average peak value per second was evaluated by laboratory virtual instrument engineering workbench (LabVIEW) to integrate it into one-minute reading. The availability of beacon measurements in a year is about 96.2%. The remaining percentage of 3.8% is meant for equipment maintenance.

The rain accumulation and rain rate based on time series were recorded from an AWS rain gauge incorporated with AWS sited in the same garden with the outdoor unit of the beacon measurement. The measurement traversed for a period of 2 years (from January 1, 2018, to December 31, 2019). The rain gauge has a diameter of 200 mm with a calibration of about 0.05 cm for each of the tips of rainfall. The equipment has an error of about 6.8% for any rain rate larger than the amount of 5 mm/h. The data logger records the rain values every 10 seconds and is integrated at the interval of 1 minute. The availability of the rain gauge in a year is about 98.6%, the remaining percentage of 1.4% is meant for equipment maintenance.

**2.2. Data processing**

Rain rate and RbA are concurrently measured throughout the observation. Only rainy days are considered in this work and any rain rate less than 0.5 mm/h is not considered. During the preprocessing of the data collected, the beacon data was synchronized with the meteorological data and an ordinary timestamp was assigned to it. Data reduction was done by removing the instrumental drifts and evaluating the attenuation reference level using the spectrum analyzer on complementary measurements. The RbA in dB is estimated using the difference between the receiving signal levels during clear sky ( $RSL_{clear\ sky}$ ) and the receiving signal levels during rainy days ( $RSL_{rainy\ day}$ ).

$$RbA (dB) = RSL_{clear\ sky} - RSL_{rainy\ day} \tag{1}$$

**2.3. Synthetic storm technique (SST)**

The synthetic storm technique (SST) is a unique algorithm that can convert rain rate-time profiles at a specific point to rain distance profiles at a specific time. It's also a powerful tool that can generate time series statistics of RbA using the time series of rain rates at the specified location [8], [25]. The SST described the value of rainfall as a function of the length where that rain moved on the line because of the wind at a special speed [28]. For high values of storm speed, it is obvious that the duration of the predicted rain-attenuation time series is near the period of the actual rain attenuation. As a result, different rainstorms might still be evaluated to determine the effect on RbA as considered in this study. Figure 1 depicts a typical illustration of the satellite link geometry and the parameters in the SST model with two layers of precipitation.

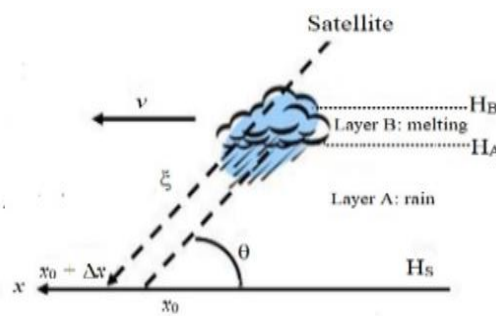


Figure 1. Typical illustration of the satellite link geometry and the parameters in the SST model with two layers of precipitation [8], [25]

During every sampling period, the attenuation by rain is estimated as the summation of specific attenuation (dB/km) multiplied by the length of the segment, as expressed in (2):

$$A_m = \sum_{j=0}^{n-1} kR_{m-j}^\alpha x(V_t \times t)_j \tag{2}$$

where  $k$  and  $\alpha$  denotes the coefficient related to the frequency of wave depolarization, temperature and drop size distribution-relating rainfall rate to the specific rain attenuation (dB/km);  $R$  is the  $m$ -th sample of the rain

rate measurement,  $m$  is the number of segments that constituted the link;  $V_t$  is the wind on a line and  $t$  is the integration time of 1-min, which is the length of the  $m$ -th segment of the link. Detailed physical and mathematical fundamentals are described at length by Matricciani [28] and updated by Kanellopoulos *et al.* [5] and therefore not repeated here.

The vertical structure of the precipitation medium has been modeled with two layers of different depths. The layer  $A$  starts from the ground with the existence of rain with a water temperature of 20 °C [29] and layer  $B$  with melting hydrometeors at 0 °C [30] as depicted in Figure 1.  $R_A$  is the homogeneously falling rain at layer  $A$ , while  $R_B$  is the apparent rain rate of layer  $B$  dominated by ice, where

$$R_A = rR_B \text{ with } r = 3.134 \quad (3)$$

the recent ITU-R rain height has also been taken into account [31]. The input parameters needed by the SST model in our region are considered as follows. The altitude above sea level of the earth station  $H_S$  is 0.008 km. According to ITU-R [31], the height of the precipitation (rain and melting layer) above sea level,  $H_B$  is 5 km and depends on the latitude ( $\phi$ ) of the earth station, where  $\phi < 23^\circ$ .

The thickness of the melting layer ( $h$ ) is 0.4 km regardless of the latitude. The NIGCOMSAT-R1 with its service footprint links at an elevation angle of 42.5° is assumed in this work. Hence the specific attenuation at a given point is converted into signal attenuation,  $A(x_0)$  for a satellite path as it is in our case using (4):

$$A(x_0) = k_A \int_0^{L_A} R^{\alpha A}(x_0 + \Delta x_0, \xi) d\xi + k_B r^{\alpha B} \int_{L_A}^{L_B} R^{\alpha B}(x_0, \xi) d\xi \quad (4)$$

where  $\xi$  is the distance measured along the satellite path.  $H_A$ , of the upper limit of layer  $A$  is given by (5).

$$H_A = H_B - h = 4.0825 \text{ km} \quad (5)$$

The radio path lengths are calculated using (6):

$$L_A = \frac{H_A - H_S}{\sin(\theta)} \text{ and } L_B = \frac{H_B - H_S}{\sin(\theta)} \quad (6)$$

where  $\theta$  is the link elevation angle;  $\Delta x_0$  is a shifting parameter that accounts for the fact that the radio path exists layer B at  $x_0 + \Delta x_0$  and can be expressed as (7):

$$\Delta x_0 = L_B - L_A = \frac{h}{\sin(\theta)} \cdot \cos(\theta) = \frac{h}{\tan(\theta)} \quad (7)$$

each of the time series of attenuation time series is then obtained from the corresponding time series rain rate by applying a fourier series to (4). Table 1 presents some of the location-based parameters used in the SST. The attenuation generated via the SST is compared with the measured attenuation and thereafter, the influence of wind speed is assessed at Ku-band over the earth-satellite links. The  $k$  and  $\alpha$  for 20 °C are deduced from [29], while at 0 °C was deduced from [30].

Table 1. Location-based parameters used for the SST [25]

Location	Latitude (°N)	Longitude (°E)	Altitude (m)	Annual mean rainfall (mm)	Frequency (12.245 GHz)			
					$k$ (20 °C)	$\alpha$ (20 °C)	$k$ (0 °C)	$\alpha$ (0 °C)
Akure	7.17	5.18	358	1524	0.0235	1.1505	0.2200	1.1668

### 3. RESULTS AND DISCUSSION

This section presents the results generated from the experimental setup and SST. It mainly presents discussions of the relevant results as well as how the results affect Ku-band signals propagating through the earth-satellite links in Nigeria. The section includes information about the rain accumulation, the cumulative distribution of rain rate, RbA beacon measurement, and the influence of wind speed on rain attenuation.

#### 3.1. Rain accumulation

In this study, the dry seasons are subdivided into the cessation period (october to november), and dry months (december to february). The wet seasons are subdivided into the commencement of the rain period (middle march to april) and rainy months (may to september). The monthly statistics of the number of occurrences of rain accumulation, rain rate, and the RbA for 2018 and 2019 were determined and presented in Table 2. Table 3 also presents the summary of the statistical events based on the monthly and seasonal variation

of the parameters. It can be seen that the quantity of rain rate relatively determines the RbA for each of the months and seasons. Although the volume of precipitation in 2018 is more than that of 2019, the number of rainy days in 2019 is more than that in 2018. This depicts that radio signals will be more attenuated in 2019 when compared with 2018.

Table 2. Monthly statistics of rain accumulation, rain rate and RbA for 2018 and 2019

Months	Volume of Rainfall (mm)	2018				No. of Rainy days	Volume of Rainfall (mm)	2019				No. of Rainy days
		Rain Rate (mm/h)		Rain Attenuation (dB)				Rain Rate (mm/h)		Rain Attenuation (dB)		
		Min	Max	Min	Max			Min	Max	Min	Max	
January	0.0	0.0	0.00	0.00	0.00	0	0.0	0.0	0.00	0.00	0	
February	0.0	0.0	0.00	0.00	0.00	0	20.4	0.8	5.46	1.54	1.89	1
March	66.0	0.8	123.80	0.18	55.85	5	77.2	0.8	10.31	0.18	3.22	11
April	11.4	0.8	76.80	0.18	18.58	1	104.4	0.8	129.4	0.18	58.78	12
May	98.6	0.8	149.60	0.18	69.50	12	178.6	0.03	180	0.01	86.07	14
June	34.0	0.8	114.00	0.18	50.78	2	93.1	0.03	225.81	0.01	91.88	15
July	148.6	0.8	125.20	0.18	56.58	16	77.5	0.03	122.6	0.01	51.54	18
August	132	0.8	140.40	0.18	64.59	13	31.3	0.03	4.09	0.01	1.12	15
September	202.2	0.8	174.60	0.18	83.09	19	72.1	0.03	6.21	0.01	1.81	13
October	77.6	0.8	174.60	0.18	83.09	14	7.8	0.03	4.32	0.01	1.20	5
November	19.2	0.8	92.20	0.18	39.76	4	1.3	0.03	2.06	0.01	0.52	2
December	0.0	0.0	0.00	0.00	0.00	0	0.0	0.0	0.00	0.00	0	
Total	789.6					86	663.7					106

Table 3. Seasonal variation of rain accumulation, rain rate and RbA

Seasons	Months	2018				No. of Rainy days	Volume of Rainfall (mm)	2019				No. of Rainy days	
		Rain Rate (mm/h)		Rain Attenuation (dB)				Rain Rate (mm/h)		Rain Attenuation (dB)			
		Min	Max	Min	Max			Min	Max	Min	Max		
Dry months	Dec-Feb	0.0	0.0	0.0	0.0	0.0	0	20.4	0.8	122.6	0.18	55.23	1
Commencement of rain period	Mar-April	77.4	0.8	123.8	0.18	55.85	6	181.6	0.8	225.8	0.18	111.89	23
Rainy months	May-Sept	615.4	0.8	174.6	0.18	83.00	62	452.6	0.03	180	0.01	86.07	75
Cessation period	Oct-Nov	96.8	0.8	174.6	0.18	83.09	18	9.1	0.03	4.32	0.01	1.19	7
Total		789.6					86	663.7					106

Figure 2 depicts the rainfall accumulation distributions over the study period. Figures 2(a) and (b) show the monthly and seasonal distributions of rainfall accumulation for the 2 years of measurements, respectively. From the result, rainfall accumulation was lowest during the dry season for both years. In the dry months, 2018 had no rain events while 2019 had a rain event with a total rainfall amount of about 20.4 mm. The rainfall accumulation in the cessation period was 96.8 mm in 2018 and 9.1 mm in 2019. The highest rainfall season was observed to be in the wet season for both years. The rain accumulation in the rainy months was 615.4 mm in 2018 and 452.6 mm in 2019. At the commencement of the rain period, the rain accumulation was 77.4 mm and 181.6 mm in 2018 and 2019, respectively. In 2018, September recorded the highest monthly rain accumulation of about 202.2 mm, while may had the highest monthly rain accumulation, about 178.6 mm, in 2019. Based on the statistics, it could be said that there would be more signal attenuation between may and September with more significant attenuation during may, July, and September. Better signal quality will be experienced around December to February. However, in 2019, March showed a high rainfall accumulation, which agrees with the work reported in Ojo *et al.* [6] that rainy seasons can vary in length, occurrence, and severity in tropical locations. Generally, the monthly distributions show most of the rainy events to be convective; this event is associated with very high levels of signal degradation. This is very crucial for determining the quality objectives of link budgeting for telecommunication systems.

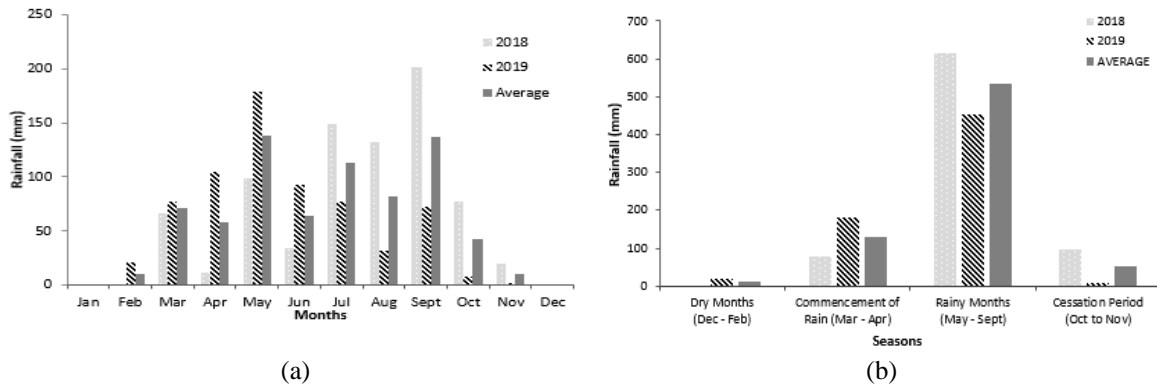


Figure 2. Distribution of rainfall accumulation for the years of measurements (a) monthly and (b) seasonal

### 3.2. Cumulative distributions of rain rate

Figure 3 depicts the intercomparison of the cumulative distribution of rain rate over the study period. Figure 3(a) presents the annual cumulative distribution of rain rate for the two years of measurements. It was observed that the yearly statistics for 2018 follow closely with those of 2019 and present a good fit at higher percentages of time up to around 0.2% with rain rates (lower than 160 mm/h). However, relatively low differences are obtained at lower percentages of time (lower than 0.004%). At 0.01% unavailability of time, the mean rain rate over the two years is about 104 mm/h, while ITU values recorded a rain rate of about 144 mm/hr. This implies that the ITU rain rate value overestimated the actual value, with an average relative error of about 28%. Figure 3(b)-(d) shows the seasonal cumulative distribution of rain rates for 2018, 2019, and the two years together, respectively. Generally, the rain rate increases as the time percentage decrease. It is noted that there is no rain recorded for the dry months in 2019, while the dry months appear as the season that experiences the lowest rain rate. In 2018 (Figure 3(b)), the rainy months take the lead, followed by the commencement of the rainy period, while the dry months take the least. However, in 2019 (Figure 3(c)), the commencement of the rainy period takes the lead, while the rainy months follow suit, and the cessation period takes the least. In Figure 3(d), the rainy months take the lead while the commencement of the rainy period follows suit, then the cessation period and the least distributions were observed in dry months. The analysis depicts the dynamic nature of rain in the region. This analysis is crucial for estimating the fade margin needed for the quality of signals since it depends on the quantitative values of rain rate and consequently determines the attenuation [32].

### 3.3. RbA-beacon measurements

Based on beacon measurements, Figure 4 presents a typical interrelated result of the measured rain rate events and the received signal levels on a rainy day (5<sup>th</sup> may 2019). Generally, it is observed that as the rain rate values increase, while the corresponding received signal level (RSL) value decreases. That is, higher rainfall is indicated by higher attenuation of signal power. Also, the duration of intense rain lasts shorter than the duration of the rain attenuation. The dynamic range of the receiver varies between -33.3 dBm and -83.2 dBm, and the received signal strength experiences deep fade during heavy rain with a rain rate of about 116 mm/hr. The rain attenuation may be more significant than 20 dB during heavy rain over satellite links in the area.

Figure 5 shows the complementary distribution function (CDF) of the RbA for the two years of measurements compared with attenuation generated using SST and the ITU-R model. It was observed that the yearly statistics follow the same trend as the CDF for rain rate as presented previously in Figure 3(a). It was observed that the yearly statistics for 2018 RbA follow closely with that of 2019 and present a good fit at higher percentages of time up to around 0.08% with rain attenuation lower than 20 dB. However, relatively low differences are obtained at lower percentages of time (lower than 0.005%). At 0.01% unavailability of time, the mean RbA over the two years is about 50 dB, while SST values recorded rain attenuation of about 51.23 dB. This implies that the SST value relatively fits the measured values with an average relative error (ARE) of about 3%. However, the rain attenuation obtained using the ITU-R model overestimated the measured values by about 16%. Table 4 presents the summary of the model's performance based on metric measures, the root mean square (RMS), average relative error (ARE), coefficient of variation (CV), and standard deviation (STD). The SST model provides the least ARE, RMS, STD, and CV averaged over the selected percentages of time. The SST model is therefore adjudged to outperform the ITU-R model based on this study.

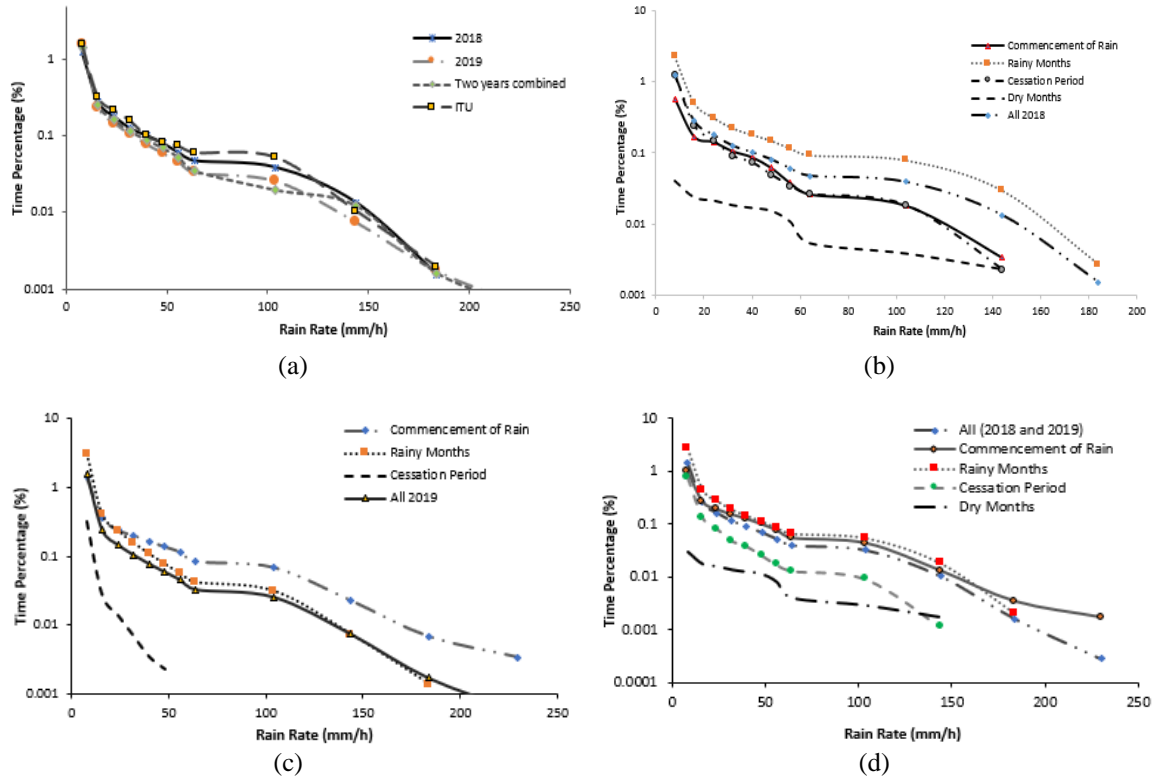


Figure 3. Intercomparison of the cumulative distribution of rain rate for (a) the years of measurement and the ITU rain rate (b) 2018 seasonal, (c) 2019 seasonal, and (d) the two years seasonal

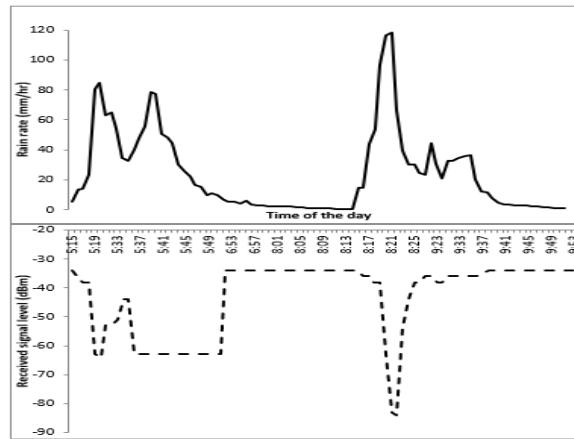


Figure 4. A typical time series of measured rain rate and the variation of measured received signal level

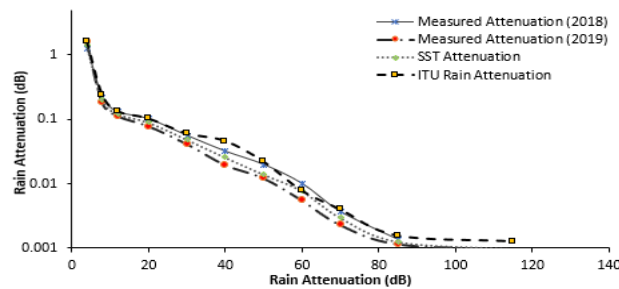


Figure 5. CDF of rain attenuation for the 2-year measurement and comparison with SST and ITU RbA

Table 4. Summary of the performance assessment of the predicted model based on metric measures

Models	ARE (%)	RMS	STD	CV
SST	3.52	3.34	32.64	0.75
ITU-R	16.05	6.56	35.07	0.77

### 3.4. Time series rain rate and rain attenuation

The time-series of the measured rain rate and the RbA based on the SST during different typical rain events is presented in Figure 6. Figures 6(a)-(e) present the time series rain rate during different typical rain events at different seasons and the rain attenuation generated by the SST. It was observed that the measured rain rate patterns show a strong correlation with the rain attenuation generated using the SST. Typically, the duration of the rain rate was the same as the duration of the generated rain attenuation time series for each of the rain events. As also presented in Figure 6(d), higher rain rate intensities such as 180 mm/h, may cause a strong RbA of about 86 dB. Such a degree of signal degradation is sufficient to severely impair the earth-satellite links or cause a total outage to the satellite services. Hence, it is imperative to adopt a technique such as a site diversity technique to mitigate the total link outages in this region.

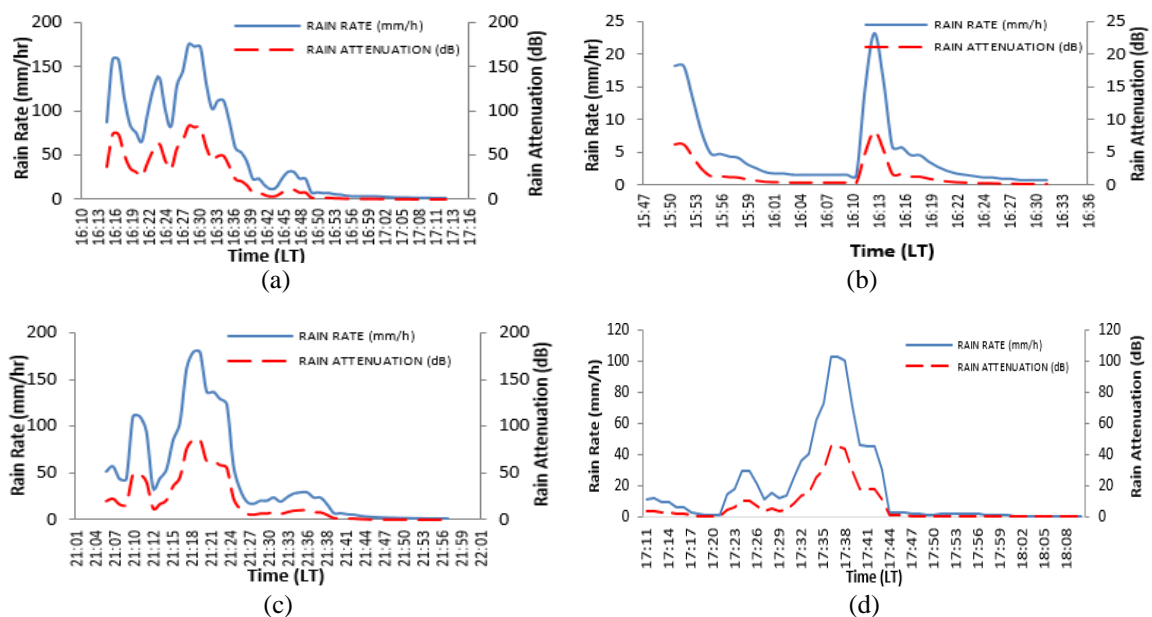


Figure 6. Time series of measured rain rate and RbA generated using the SST during different typical rain events on (a) 7<sup>th</sup> Mar. 2018, (b) 24<sup>th</sup> Sep. 2018, (c) 27<sup>th</sup> Nov. 2018, (d) 5<sup>th</sup> May 2019; and (e) 30<sup>th</sup> Jun. 2019

### 3.5. Influence of wind speed on rain attenuation

Here, further analysis was carried out to assess the influence of wind speed on time series attenuation. The first subsection characterizes both wind speed and wind direction, while the second and the third subsections investigate the likelihood of wind speed occurrence during various rain events, and the analysis of the measured rain attenuation and the wind speed, respectively. The last subsection also discusses the rain-based attenuation at different wind speeds.

#### 3.5.1. Characterizing wind direction and wind speed

Figure 7 also depicts the results of the characterization of the wind directions and wind speeds based on the season of the year. Figure 7(a)-(c) presents the wind directions and wind speeds for the wet season (2018), dry season (november 2018 to March 2019), and wet season (2019) observations. It was observed that for the majority of the total % of time, the wind speed was below 4.1 m/s in all the seasons. In the wet season (2018), the three dominant wind directions are SE, ESE, and E, with 7.85%, 7.26%, and 6.42% of the time respectively. This implies that the direction SE and ESE have more impact on the level of signal degradation, especially during the season. Also, in the dry season, the three dominant wind directions are W, SE, and E with 16.56%, 12.38%, and 9.60% of the time, respectively. While in the wet season (2019), the three dominant wind directions are E, ESE, and W with 8.67%, 7.48%, and 7.31% of the time, respectively. Also, the direction SE



and ESE will contribute more to signal degradation when compared to W based on the % occurrences. According to the seasonal assessment, the dry season has the highest occurrence of the wind speed and direction.

**3.5.2. Probability occurrence of wind speed for all rain events**

Figure 8 presents the probability distribution of wind speed for all rain events in 2018 and 2019. It was observed that the maximum value of wind speed was below 8 m/s during 88% of rain events. During this same period, the average wind speed was less than or equal to 5 m/s.

**3.5.3. Measured rain attenuation and wind speed at different rain events**

The influence of the wind speed on time-series measured RbA during different typical rain events is also presented in Figure 9. Figure 9(a)-(f) presents the measured rain attenuation and the related wind speed for some selected rain events. It was observed in all the typical rain events that although the duration pattern for both the rain attenuation and wind speed looked similar, the rain attenuation peaks do not synchronize with the wind speed peaks, indicating a sporadic correlation between rain attenuation and wind speed. Generally, the influence of the wind speed seems to be very minimal on the RbA, especially during the rainy period.

**3.5.4. Rain-based attenuation at different wind speed**

The time series rain attenuation and predicted rain attenuation by SST as a function of wind speed for typical rain events is depicted in Figure 10. For example, Figure 10(a) shows the predicted rain attenuation by SST as a function of wind speed at 1.0 m/s, 1.5 m/s, 2.0 m/s, 3.0 m/s, and 4.0 m/s for a typical rain event of 7th March 2018 for about 30 minutes. The predicted rain attenuation by SST as a function of wind speed at 1.0 m/s, 1.5 m/s, 2.0 m/s, 3.0 m/s, and 4.0 m/s for a tropical rain event on 27th April 2019 for about 50 minutes was also presented in Figure 10(b). It is generally observed that the predicted rain attenuation increases with an increase in the variation of the wind speed.

The CDF of rain attenuation and predicted rain attenuation by SST for different wind speed is presented in Figure 11. For example, the CDF of RbA at different wind speeds (0.5 m/s, 1.0 m/s, 1.5 m/s, 2.0 m/s, 2.5 m/s, 3.0 m/s, 3.5 m/s and 4.0 m/s) for 2018 and 2019 is shown in Figure 11(a) and 11(b) respectively. It was observed that although rain attenuation CDF at the different wind speeds follows closely and gives a good fit, the predicted rain attenuation CDF also increases with an increase in the variation of the wind speed.

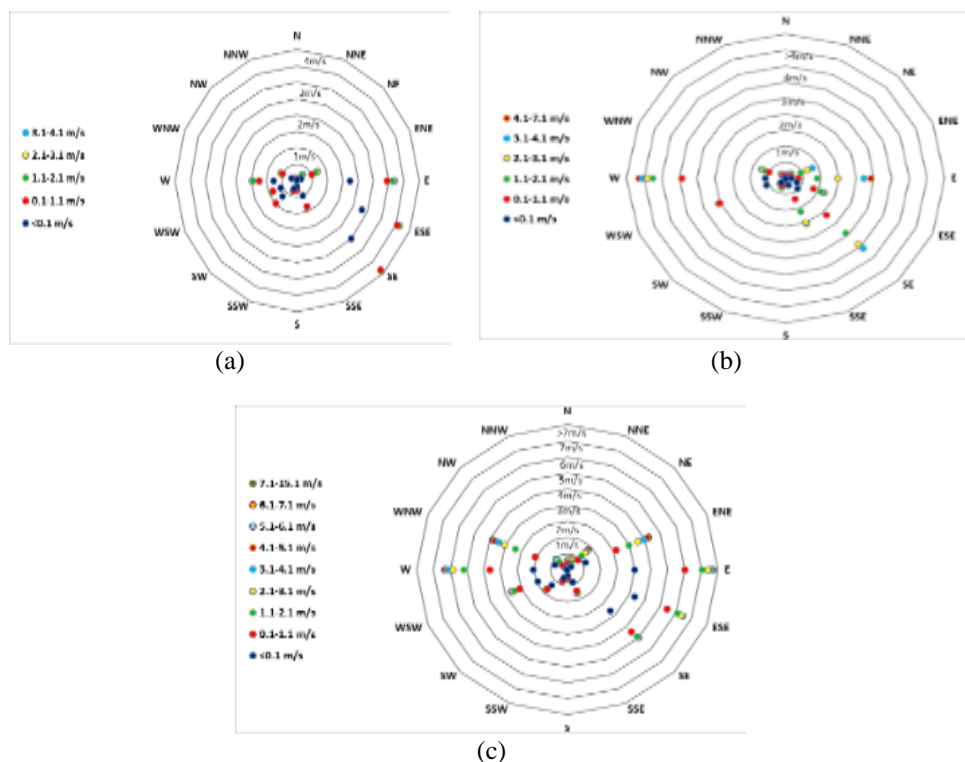


Figure 7. Characterizing the wind directions and wind speeds for (a) Wet season (2018), (b) dry season (November 2018 to March 2019), and (c) wet season (2019)

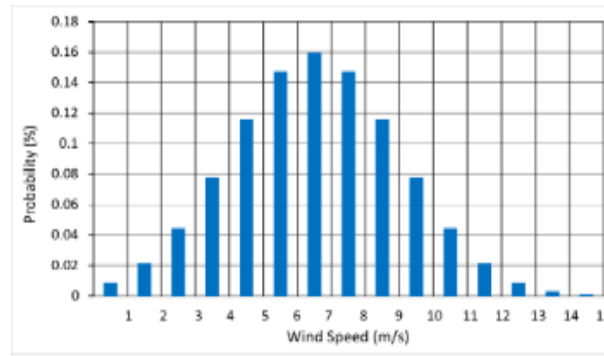


Figure 8. Probability distribution of wind speed for all rain events measured in 2018 and 2019

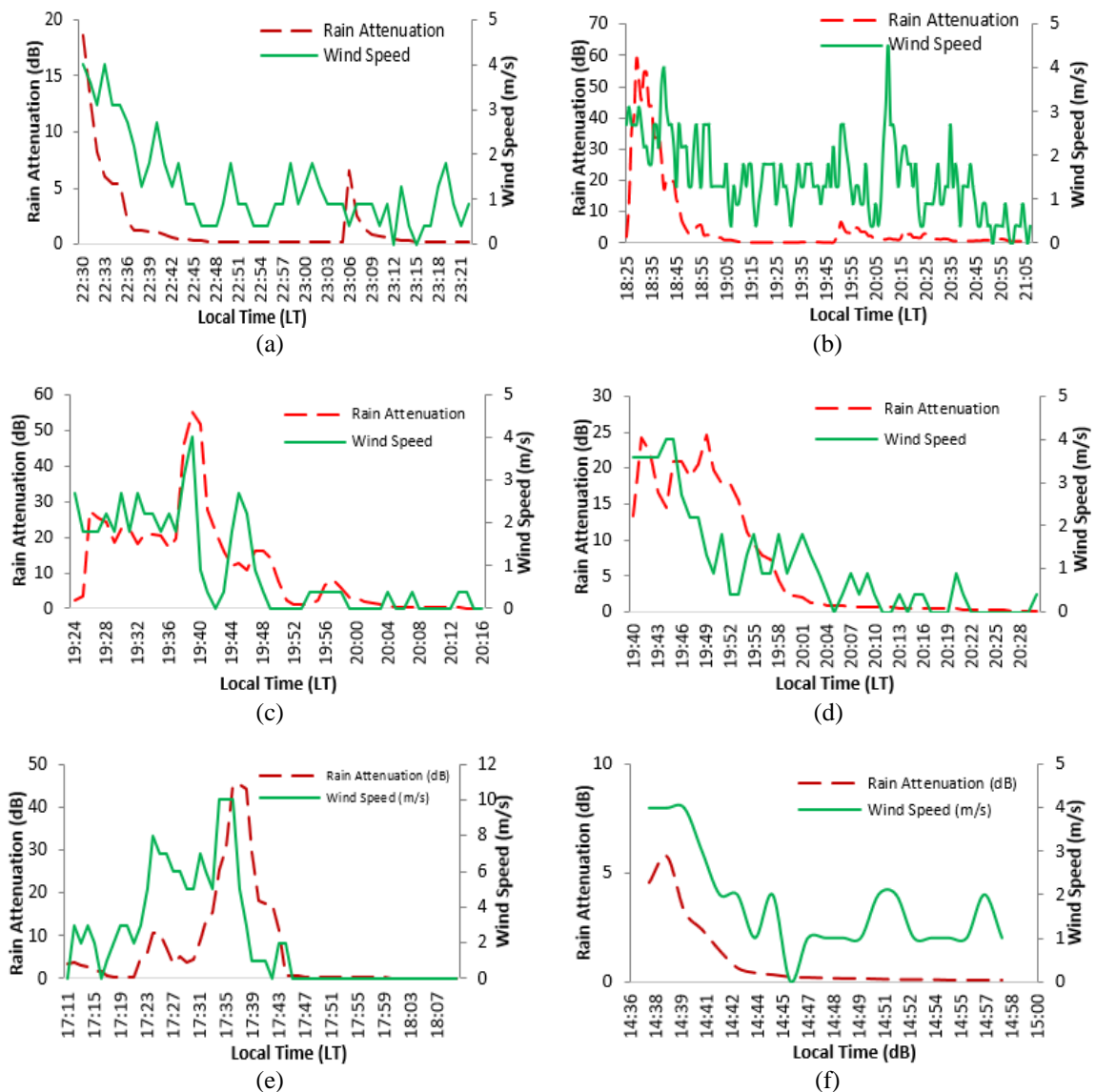


Figure 9. Influence of wind speed on time series measured RbA during different typical rain events (a) 14<sup>th</sup> April 2018, (b) 5<sup>th</sup> May 2018, (c) 27<sup>th</sup> February 2019, (d) 5<sup>th</sup> March 2019, (e) 30<sup>th</sup> June 2019, and (f) 10<sup>th</sup> October 2019

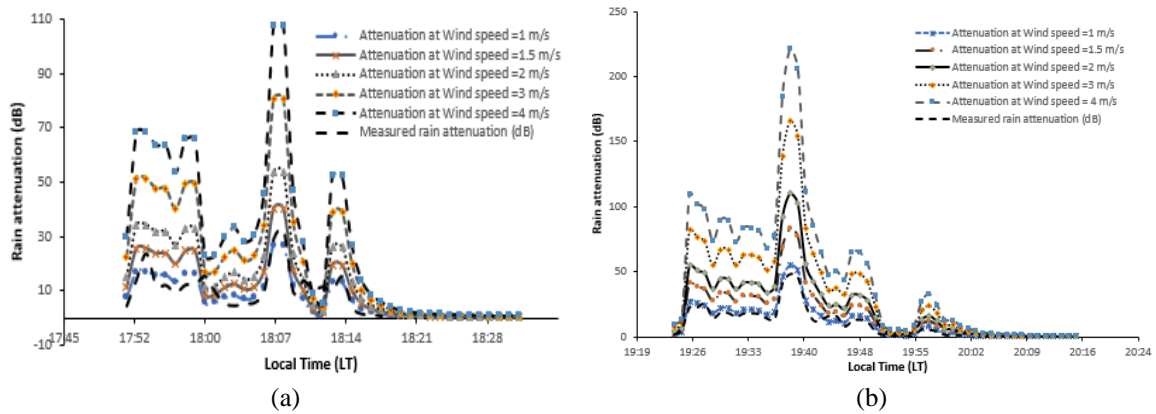


Figure 10. Time series rain attenuation and predicted rain attenuation by SST as a function of wind speed for typical rain events of (a) 7<sup>th</sup> March 2018 and (b) 27<sup>th</sup> April 2019

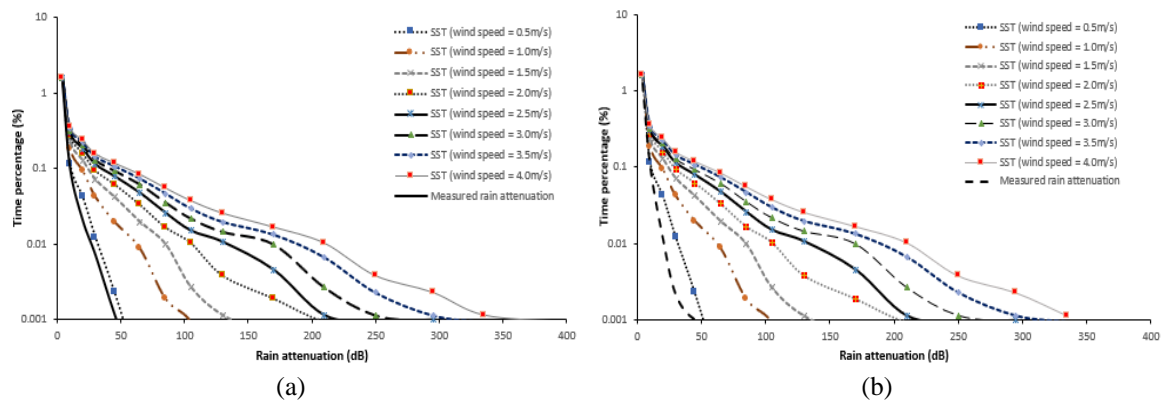


Figure 11. CDF of rain attenuation and predicted rain attenuation by SST for different wind speed in (a) 2018 and (b) 2019

**4. CONCLUSION**

The rainfall accumulation, rain rate, wind speed, wind direction, and RbA were concurrently measured for two years in a tropical location (Akure), Nigeria, on the Ku-band satellite-to-Earth path. The SST algorithms were also validated over the slant path Ku-band signals at different wind speeds. Further analysis was carried out to assess the impact of wind speed on time series attenuation in the Ku-band. Analysis of the average and total monthly accumulation shows the significance of the months with more volume of water (between May and September). As more volume of water is observed in these months is a signal to the system engineers to prepare for mitigating measures to enhance the good quality objectives of telecommunication systems. It was observed that the measured rain rate shows a strong correlation in trend with the SST generated RbA based on the lowest metric measures when compared with the ITU-R model and the duration of the measured rain rate was the same as the duration of the generated RbA time series for each of the rain events considered. Predicted rain attenuation as a function of wind-speed variations by SST shows a minimal effect on this region. Although the duration pattern RbA and wind speed look similar, most of the rain attenuation peaks do not synchronize with the wind speed peaks. It is generally observed that the predicted rain attenuation and rain attenuation CDF increase with an increase in the variation of the wind speed. It can be generally inferred that the results based on this work will provide essential information to system designers for suitable site diversity measures to improve link availability and proper communication system planning at different seasons in Nigeria.

**REFERENCES**

[1] S. Malisuwan, J. Sivaraks, N. Madan, and N. Suriyakrai, "Design of microstrip patch antenna for Ku-Band Satellite communication applications," *International Journal of Computer and Communication Engineering*, vol. 3, no. 6, pp. 413–416, 2014, doi: 10.7763/ijcce.2014.v3.360.




[2] A. K. Lwas, M. R. Islam, M. H. Habaebi, S. J. Mandeep, A. F. Ismail, and A. Zyoud, "Effects of wind velocity on slant path rain-attenuation for satellite application in Malaysia," *Acta Astronautica*, vol. 117, pp. 402–407, Dec. 2015, doi: 10.1016/j.actaastro.2015.09.008.

- [3] G. A. Siles, M. Heredia, and R. Harriague, "Cloud detection models and their effect on the calculation of cloud attenuation: Assessment at Ka-and Q-band at 4065 meters of altitude," in *2020 14th European Conference on Antennas and Propagation (EuCAP)*, Mar. 2020, pp. 1–5, doi: 10.23919/EuCAP48036.2020.9135558.
- [4] A. Dissanayake, J. Allnutt, and F. Haidara, "A prediction model that combines rain attenuation and other propagation impairments along Earth-satellite paths," *IEEE Transactions on Antennas and Propagation*, vol. 45, no. 10, pp. 1546–1558, 1997, doi: 10.1109/8.633864.
- [5] S. A. Kanellopoulos, A. D. Panagopoulos, E. Matricciani, and J. D. Kanellopoulos, "Annual and diurnal slant path rain attenuation statistics in Athens obtained with the synthetic storm technique," *IEEE Transactions on Antennas and Propagation*, vol. 54, no. 8, pp. 2357–2364, 2006, doi: 10.1109/TAP.2006.879209.
- [6] J. S. Ojo, M. O. Ajewole, and S. K. Sarkar, "Rain Rate and rain attenuation prediction for satellite communication in Ku and Ka bands over Nigeria," *Progress In Electromagnetics Research B*, vol. 5, pp. 207–223, 2008, doi: 10.2528/PIERB08021201.
- [7] J. S. Mandeep, "Comparison of rainfall models with Ku-band beacon measurement," *Acta Astronautica*, vol. 64, no. 2–3, pp. 264–271, Jan. 2009, doi: 10.1016/j.actaastro.2008.06.026.
- [8] H. Y. Lam, L. Luini, D. J. A. D. Panagopoulos, and C. Capsoni, "Preliminary analysis of ITU-R rain attenuation time series synthesizers in equatorial Kuala Lumpur," in *2011 IEEE International RF & Microwave Conference*, Dec. 2011, pp. 298–302, doi: 10.1109/RFM.2011.6168753.
- [9] L. J. Ippolito, *Radiowave propagation in satellite communications*. Dordrecht: Springer Netherlands, 1986.
- [10] G. A. Siles, M. Heredia, and R. Harriague "Cloud detection models and their effect on the calculation of cloud attenuation: Assessment at Ka-and Q-band at 4065 meters of altitude". In *2020 14th European Conference on Antennas and Propagation (EuCAP)*, pp. 1-5, March 2020, IEEE. doi: 10.1088/1742-6596/1874/1/012011
- [11] S. Chakraborty, M. Chakraborty, and S. Das, "Experimental studies of slant-path rain attenuation over tropical and equatorial regions: a brief review," *IEEE Antennas and Propagation Magazine*, vol. 63, no. 3, pp. 52–62, Jun. 2021, doi: 10.1109/MAP.2020.2976911.
- [12] M. O. Fashuyi and T. J. Afullo. "Rain attenuation prediction and modeling for line-of-sight links on terrestrial paths in South Africa" *Radio Science*, Vol. 42, , 2007. RS5006, doi:10.1029/2007RS003618
- [13] E. O. Olurotimi, O. Sokoya, J. S. Ojo, and P. A. Owolawi, "Observation of bright-band height data from TRMM-PR for satellite communication in South Africa," *Journal of Atmospheric and Solar-Terrestrial Physics*, vol. 160, pp. 24–33, Jul. 2017, doi: 10.1016/j.jastp.2017.05.004.
- [14] S. Das and A. R. Jameson, "Site diversity prediction at a tropical location from single-site rain measurements using a bayesian technique," *Radio Science*, vol. 53, no. 6, pp. 830–844, Jun. 2018, doi: 10.1029/2018RS006597.
- [15] P. Panchal and R. Joshi, "Performance analysis and simulation of rain attenuation models at 12–40 GHz band for an earth space path over Indian cities," *Procedia Computer Science*, vol. 79, pp. 801–808, 2016, doi: 10.1016/j.procs.2016.03.110.
- [16] J. S. Ojo, E. O. Olurotimi, and O. O. Obiyemi, "Assessment of total attenuation and adaptive scheme for quality of service enhancement in tropical weather for satellite networks and 5g applications in Nigeria," *Journal of Microwaves, Optoelectronics and Electromagnetic Applications*, vol. 20, no. 2, pp. 228–247, Jun. 2021, doi: 10.1590/2179-10742021v20i21064.
- [17] G. N. Ezeh, N. S. Chukwunke, N. C. Ogujiofor, and U. H. Diala, "Effects of rain attenuation on satellite communication link," *Advances in Science and Technology Research Journal*, vol. 8, nr. pp. 1–11, 2014, doi: 10.12913/22998624.1105138.
- [18] J. E. Allnutt and F. Haidara, "Ku-band diurnal fade characteristics and fade event duration data from three, two-year, Earth-space radiometric experiments in Equatorial Africa," *International Journal of Satellite Communications*, vol. 18, no. 3, pp. 161–183, 2000, doi: 10.1002/1099-1247(200005/06)18:3<161::AID-SAT653>3.0.CO;2-#.
- [19] ITU-R PN.837-1 RECOMMENDATION, "Characteristics of precipitation for propagation modelling," *International Telecommunication Union*, vol. 1, pp. 1–4, 1994.
- [20] M. Tamrakar, K. Bandyopadhyay, and A. De, "Comparison of rain attenuation prediction models with ku-band beacon measurement for satellite communication system," in *2010 International Conference on Signal Processing and Communications, SPCOM 2010*, Jul. 2010, pp. 1–5, doi: 10.1109/SPCOM.2010.5560497.
- [21] S. L. Jong, H. Y. Lam, J. Din, and M. D'Amico, "The relationship between ground wind direction and seasonal variation of rain attenuation at Ku band satellite broadcasting services," in *2014 XXXIth URSI General Assembly and Scientific Symposium (URSI GASS)*, Aug. 2014, pp. 1–4, doi: 10.1109/URSIGASS.2014.6929042.
- [22] S. T. Ogunjo, J. B. Dada, and O. O. Elijah, "Investigation of wind parameters at an akure station," *International Journal of Science and Society*, vol. 3, no. 1, pp. 39–51, 2013.
- [23] L. Luini *et al.*, "Weather radar data for site diversity predictions and evaluation of the impact of rain field advection," *International Journal of Satellite Communications and Networking*, vol. 29, no. 1, pp. 79–96, 2011, doi: 10.1002/sat.953.
- [24] X. X. Zhao, Y. H. Lee, and O. J. Teong, "Effect of diurnal variations of rainfall in satellite systems at Ku and Ka band in Singapore," in *2010 Asia-Pacific Microwave Conference*, 2010, pp. 1950–1953.
- [25] J. S. Ojo and O. C. Rotimi, "Diurnal and seasonal variations of rain rate and rain attenuation on Ku-band satellite systems in a tropical region: a synthetic storm techniques approach," *Journal of Computer and Communications*, vol. 03, no. 04, pp. 1–10, 2015, doi: 10.4236/jcc.2015.34001.
- [26] R. Nalinggam, W. Ismail, and J. S. Mandeep, "Rain-induced attenuation for Ku-band satellite communications in the west coast of Peninsular Malaysia, Penang," *Annales des Telecommunications/Annals of Telecommunications*, vol. 67, no. 11–12, pp. 569–573, 2012, doi: 10.1007/s12243-012-0300-4.
- [27] M. R. Islam, Asma A. H. Budalal, M. H. Habaebi, K. Badron and A. F. Ismail. "Performance analysis of rain attenuation on earth-to-satellite microwave links design in Libya," in IOP Conference Series: Materials Science and Engineering, Volume 260, 6th Int 10.1088/1757-899X/260/1/012041 International Conference on Mechatronics - ICOM'17 8–9 August 2017, Kuala Lumpur, Malaysia, doi: 10.2528/PIERM14083003.
- [28] E. Matricciani, "Physical-mathematical model of the dynamics of rain attenuation based on rain rate time series and a two-layer vertical structure of precipitation," *Radio Science*, vol. 31, no. 2, pp. 281–295, Mar. 1996, doi: 10.1029/95RS03129.
- [29] ITU-R Recommendation P.838-3, "Specific attenuation model for rain for use in prediction methods," *International Telecommunication Union*, no. 2, pp. 1–2, 1999, [Online]. Available: [https://www.itu.int/dms\\_pubrec/itu-r/rec/p/R-REC-P.838-3-200503-I!!PDF-E.pdf](https://www.itu.int/dms_pubrec/itu-r/rec/p/R-REC-P.838-3-200503-I!!PDF-E.pdf).
- [30] D. Maggiori, "Computed transmission through rain in the 1–400 GHz frequency range for spherical and elliptical drops and any polarization," *Alta frequenza*, vol. 50, no. 5, pp. 262–273, 1981.
- [31] ITU-R Recommendation P.839-4, "Rain height model for prediction methods," *International Telecommunication Union*, vol. 4, pp. 1–3, 2013.




- [32] A. Z. Papafragkakis, C. I. Kouroriorgas, and A. D. Panagopoulos, "Performance of micro-scale transmission & reception diversity schemes in high throughput satellite communication networks," *Electronics*, vol. 10, no. 17, p. 2073, Aug. 2021, doi: 10.3390/electronics10172073.

## BIOGRAPHIES OF AUTHORS






**Joseph Sunday Ojo**    is Associate Professor at college of Electrical & Mechanical Engineering, National is Professor of Radio and Satellite Communication Physics/Space Scientist at the Federal University of Technology, Akure, Nigeria. He Holds a PhD degree in Physics Electronics from Department of Physics at the Federal University of Technology, Akure. He is the head of the Radio and Satellite Communication Research Laboratory (RSCRL) at the Federal University of Technology of Technology, Akure, Nigeria. He is a recipient of different national and international awards such as National University Commission Award, Young Scientist Award, Regular Associate of ICTP, Italy among others. His research interests include Radio and Satellite Communication Physics, Space Physcs, Artificial Intelligence, image/signal processing, Free Space Optics, Smart Grids etc. His vast and expertise in several fields which include satellite communication, RF propagation and engineering, Microwave Engineering, Space Physics, Antennas and Propagation, Radio waves and satellite propagation, free space optics, Astrophysics among others. He has authored and co-authored over 160 reseach articles. He can be contacted at email: ojojs\_74@futa.edu.ng.



**Isaac Olawale Sunday**    received the B.Sc. degree in Physics He is presently a Master's Degree Student in Communication Physics Option of the Federal University of Technology Akure, Nigeria. His research interest is in the area of Radio wave Propagation and Satellite Communications. He can be contacted at email: hisaacolawalesunday1@gmail.com.



**Elijah Olusayo Olurotimi**    is a Researcher and Lecturer (Contract) at Department of Electronic and Computer Engineering, Durban University of Technology, South Africa. He received a Final Diploma (2005) and Post Graduate Diploma (2008) in Physics Electronics, Master of Technology (2013) in Communication Physics from the Federal University of Technology, Akure, Nigeria and Doctor of Engineering (2018) in Electrical and Computer Engineering from Durban University of Technology, South Africa. His research interests include Satellite and Radio Propagation Communication, Free Space Optics, Machine Learning, Computer Vision, Data Science, Signal/Image Processing, and Pattern Recognition, Renewable Energy, Power Electronic Systems Design, Optical Wireless Communications, Control Systems, Smart Grid, Biomedical Engineering, Space & Remote Sensing, Weather and Climate, among others. He can be contacted at email: elisayrot@gmail.com.